CrystEngComm

Accepted Manuscript

ROYAL SOCIETY OF CHEMISTRY

www.rsc.org/crystengcomm

Journal Name

ARTICLE

A new Co-nitroimidazolate-dicarboxylate pillared-layer network with various types of channels and ultra-large cages for gas uptake†

Received 00th January 20xx,
Accepted 00th January 20xx

DOI: 10.1039/x0xx00000x

www.rsc.org/crystengcomm

Xiao-Qing Guo,[ab] Miao Wang,[b] Yan-Feng Tang,[b] Fei Meng,[c] Guo-Qing Jiang*[b] and Jin-Li Zhu*[b]

A novel porous coordination polymer based on Co-nitroimidazolate-dicarboxylate pillared-layer network, namely, $[Co_7(bdc)_6(nIm)_2(H_2O)_6]\cdot 3H_2O\cdot 3DMF$, (**1**, H_2bdc = 1,4-benzenedicarboxylic acid, nIm = 2-nitroimidazole), has been synthesized by solvothermal reaction. The microporous layers of **1** are consisted of two kinds of SBUs—six-connected $Co_3(O_2CR)_6$ and three-connected $[Co_2(O_2CR)_3]^+$, forming an unprecedented Co_3-Co_2-bdc-based layers with three types of diamonded grids in the *bc* plane. The layers are further linked by bidentate-bridging nIm ligands as pillars into a 3-D metal-organic framework with two kinds of rectangular channels parallel to the *c* axis. It is worth mentioning that compound **1** also exhibits uniquely polyhedral cages with maximum diagonal dimension as long as 31.019Å, which has fallen in the scope of mesoporous (2~50nm). To systematically evaluate the channels and special cages, the adsorption ability of **1** were measured by N_2, H_2 and CO_2 sorption experiment. Topological analysis indicates that compound **1** adopts a new topological structure with point symbol of $\{4^{12}.6^{14}.8^2\}\{4^6\}_2$. Moreover, thermal gravimetric analysis (TGA) of as-synthesized **1** reveals a stability range up to 311℃.

Introduction

Porous materials such as metal-organic frameworks (MOFs) have emerged as a unique class of crystalline solid-state materials due, in part, to their fascinating molecular topologies along with potential applications in gas adsorption and separation, luminescence, catalysis, magnetism and more.[1] In the past two decades, so many chemists strived to explore new strategies and synthesize the target materials,[2] while facts have proved that the synthesis of MOFs with expectant structures and properties was very challenging. Amongst those of reported coordination polymers, there are three types of well-known MOFs—metal-carboxylate frameworks (MCFs),[3] zeolitic imidazole frameworks (ZIFs)[4] and metal-azolate frameworks (MAFs),[5] which have attracted considerable efforts to research factors influencing and determining the self-assembly processes and the properties of the resulting products. Careful selection of ditopic or polytopic organic carboxylates with different geometry, size, functionality linked with metal-containing units can effectively improve the variety and multiplicity of MCFs. MOF-5 as one of the most spectacular MCFs, which comprises $Zn_4O(CO_2)_6$ octahedral SBUs (secondary building units) and six cheating bdc^{2-} units, was reported by Yaghi group.[6a] The gas sorption measurements of MOF-5 exhibited ultrahigh porosity of 61% and BET surface area of 2320 m^2/g. ZIFs designed by Yaghi[6b] often reveal exceptional thermal and chemical stability, which is very important for practical application of porous materials. For instance, ZIF-68 [Zn(BIm)(nIm), where BIm = benzimidazole][7] shows a thermal stability range up to 390℃ and keeps unaltered after immersion in boiling water, benzene, and methanol for seven days. In recent years, MAFs have gained intensive attention as a new kind of porous materials for many reasons. Azolate ligands such as imidazole derivatives exhibit strong coordination ability in bridging metal ions.[5] Furthermore, the structures of MAFs have advantage of high thermal and chemical stability, ultra-large cages and small apertures for molecular sieving.[8]

However, is there a new way of combining the diversity of MCFs and the large cage of imidazole in the same frameworks? Our group is interested in preparing a class of porous materials that can contain the features and properties of MCFs and ZIFs simultaneously, and improve the complexity of pore composition and structure, and further impacting the gas uptake capacity and selectivity.[2b,9] Rational selection of cross-linking components (carboxylate and imidazolate segment) is critical to the formation of this multicomponent chemical system. The first step is to choose two appropriate ligands prior to performing directional and strong coordination ability in bridging metal ions. 1,4-benzenedicarboxylic acid, as a commonly ditopic organic acid, has a variety of coordination

[a] School of Textile and Clothing, Nantong University, Nantong, China.
[b] College of Chemistry and Chemical Engineering, Nantong University, Nantong, China. E-mail: jgq3518@163.com, jinlizhu@ntu.edu.cn
[c] State Key Laboratory of Coordination Chemistry, School of Chemistry and Chemical Engineering, Nanjing University, Nanjing, China.
† Electronic Supplementary Information (ESI) available: CCDC 1436248 for complex **1**. For ESI and crystallographic data in CIF or other electronic format see DOI: 10.1039/x0xx00000x

modes since each single O-donor can bind one, two, or three metal ions, and contributing to the formation of coordination polymers through the self-assemblies with metal ions (or clusters).[10] 2-nitroimidazole, as a nitro functionalized imidazole linker, has been widely used in the preparation of ZIFs (a search in the Cambridge Structural Database indicates a total of 40 hits for ZIFs based on 2-nitroimidazolate). For example, Yaghi and his co-workers[2b] have reported a series of ZIFs-n (where, n=68~70, 78~82) based on equimolar amounts of nIm and a substituted Im (Im = $C_3N_2H_3^-$, functional groups: -Cl, -CN, -Me, -Br and $–NO_2$), in which ZIF-78 shows very high CO_2 adsorption capacity and selectivity, because the nitro functional group possesses a higher dipole moment than other groups, benefiting to the dipole-quadrupole interactions with CO_2 molecules. Moreover, the $–NO_2$ group in nIm possesses an electron-withdrawing effect, indicating that nIm has higher basicity and favours to from the corresponding nitroimidazolate. In orger to overcome the propensity for producing phase separation when mixed links are used in the synthesis,[2a] the second step is to select appropriate metal ions with strong coordination affinity to both carboxylates and imidazolates. Divalent metal ions (such as Zn^{2+}, Co^{2+} ions) have been widely used in the synthesis of MCFs[11] and ZIFs[2c] exhibiting diverse coordination modes (generally, four-coordinated mode in ZIFs and five-, six-coordinated modes in MCFs).

Herein, we explore the synthesis and crystal structure of a new Co-nitroimidazolate-dicarboxylate framework, namely, $[Co_7(bdc)_6(nIm)_2(H_2O)_6]\cdot 3H_2O\cdot 3DMF$, with a 3-D pillared-layer network arising from the linking of 2-D mixed-cluster layers through bidentate-bridging nIm ligand. The structure displays various types of channels (diamond and rectangular channels) and nanometre-sized cages (maximum dimension of 3.1nm). Various types of channels structure, oversized cages and the decoration of $–NO_2$ functional group, primarily contribute to the biggish solvent-accessible volume, 16,396.1Å^3, equal to 61.3% of the unit cell volume of 26,725.8Å^3 and the outstanding CO_2 adsorption capacity. H_2 uptake as high as 1.54 wt% at 77K/1atm and CO_2 uptake of 14.5 wt% at 273K/1atm have been observed for **1**, and the BET and Langmuir surface area are 995m^2/g and 1113m^2/g, respectively. Its thermodynamic stability and gas adsorption property have also been studied.

Experimental

Materials and methods

The 2-nitroimidazole was purchased from J&K Company, and other chemicals purchased are of reagent grade and used without further purification. FT-IR spectrometer was recorded on an AVATAR360 FT-IR spectrometer using KBr pellets. Thermo-gravimetric analysis (TGA) was recorded on a NETZSCH STA 449F3 analyzer with heating rate of 10 K/min under N_2 atmosphere. Powder X-ray diffraction (PXRD) pattern was collected on a Bruker D8 Advance diffractometer with Cu Kα radiation (1.5418Å) at room temperature. The gas sorption isotherms were measured volumetrically using a Quanta-chrome Autosorb IQ surface area analyser (ASAP 2020).

Synthesis of compound 1

Preparation of $[Co_7(bdc)_6(nIm)_2(H_2O)_6]\cdot 3H_2O\cdot 3DMF$. A solid mixture of $Co(NO_3)_2\cdot 6H_2O$ (29.1mg, 0.1mmol), 1,4-benzene-dicarboxylic acid (33.2mg, 0.2mmol) and 2-nitroimidazole (22.6mg, 0.1mmol) was dissolved in DMF (3mL) in a 20mL vial to obtain a reddish solution. The vial was tightly capped and heated at a rate of 5□ /min to 100□ in a programmable oven and held at this temperature for 72h, then cooled at a rate of 0.4□/min to room temperature. Subsequently, dark red block crystals were obtained in 57% yield based on Co. Elemental Analysis (%) for $C_{54}H_{42}N_6O_{35}Co_7$ calcd: C, 35.96; H, 3.35; N, 6.29. Found: C, 36.19; H, 3.13; N, 6.10. IR (KBr, cm^{-1}): 3403 (br), 2932 (w), 1659 (s), 1590 (m), 1492 (m), 1384 (s), 1163 (w), 1101 (w), 820 (w), 750 (m), 532 (w).

Crystallographic studies

Single crystal suitable for X-ray diffraction were selected and mounted onto a thin glass fibre. The intensity data of **1** was collected on a Bruker SMART APEX II diffractometer at 296K with graphite monochromated Mo/Kα radiation (λ = 0.71073 Å). Structural solution and refinement based on F^2 was performed with the SHELXTL package.[13a] All non-hydrogen atoms were refined with anisotropic displacement parameters. Hydrogen atoms were generated geometrically. In this structure, free solvent molecules were removed using the SQUEEZE[13b] routine of PLATON[14] and the structure was then refined again using the data generated. The crystallographic data collection and refinement for **1** was summarized in Table 1. The selected bond lengths and angles are given in Table 2.

Table. 1 Crystallographic data and structure refinement for **1**.

Compound	1
Empirical formula	$C_{54}H_{42}N_6O_{35}Co_7$
Formula weight	1747.45
Temperature	296K
Crystal system	Orthorhombic
Space group	Cmca
Unit cell dimensions	a = 24.6165(9)Å
	b = 35.8569(15)Å
	c = 30.2783(12)Å
	α = β = γ = 90°
Volume	26725.8(18)Å^3
Z	8
d_{calcd} (g/cm^3)	0.869
μ (mm^{-1})	0.897
No. of measured, independent and observed [I > 2.0 σ(I)] reflections	67131, 15851, 9460
λ (Å)	0.71073
R_{int}	0.042
R_1 ($I > 2\sigma$)/ wR_2 (all data)	0.0816; 0.2494

Table. 2 Selected bond lengths (Å) and angle (°). Symmetry transformations used to generate equivalent atoms: (i) 1/2-x, y, 3/2-z.

Compound **1**			
Co1-O3	2.041(4)	Co1-O12	2.020(4)
Co1-O14	2.174(4)	Co2-N2	2.044(5)
Co2-O4	1.996(4)	Co2-O13	1.970(4)
Co2-O14	2.130(4)	Co2-O15	2.223(5)
Co3-O5	1.933(5)	Co3-O11	1.942(5)
Co3-N1	2.035(5)	Co3-O2	1.976(5)
Co4-O1	2.022(5)	Co4-O7	2.104(8)
Co4-O6	1.999(5)	Co4-O8	2.222(9)
Co4-O9	2.195(8)	Co4-O10	2.040(6)
Co1-Co2	3.3719(7)		
O3-Co1-O12	93.83(17)	O3-Co1-O14	98.59(16)
O3-Co1-O3^{i}	84.58(18)	O3-Co1-O4	84.02(16)
O12-Co1-O14	85.43(15)	O12-Co1-O12^{i}	89.76(16)
O12-Co1-O14^{i}	92.09(15)	O14-Co1-O3^{i}	84.02(16)
O4-Co2-O13	109.43(18)	O4-Co2-O14	107.97(16)
O4-Co2-O15	98.8(2)	O4-Co2-N2	93.67(18)
O13-Co2-O4	92.74(17)	O13-Co2-O15	145.7(2)
O13-Co2-N2	102.70(19)	O14-Co2-O15	59.34(17)
O14-Co2-N2	147.59(17)	O15-Co2-N2	94.38(19)
O2-Co3-O5	112.9(2)	O2-Co3-O11	106.0(2)
O2-Co3-N1	98.4(2)	O5-Co3-O11	126.5(2)
O5-Co3-N1	103.6(3)	O11-Co3-N1	105.4(2)
O1-Co4-O6	95.4(2)	O1-Co4-O7	85.8(3)
O1-Co4-O8	88.4(2)	O1-Co4-O9	174.9(2)
O1-Co4-O10	94.9(2)	O6-Co4-O7	86.0(3)
O7-Co4-O9	90.4(3)	O6-Co4-O9	87.7(3)
O6-Co4-O10	97.6(2)	O7-Co4-O8	92.7(3)
O6-Co4-O8	175.9(3)	O7-Co4-O10	176.3(3)

Results and discussion

Synthesis

In order to evaluate the role of nitro functional group in the construction of compound **1**, our group also attempted to replace 2-nitroimidazole with other imidazole derivatives (such as imidazole, 2-bromoimidazole and 2-methylbenzimidazole). However, the crystal structure similar to compound **1** failed to be obtained under various reaction conditions. As a result, we preliminary speculated that the nitro functional group may play an induced role in the self-assembly process of two-dimensionally mixed-cluster layers. In addition, the nitro group of nIm possesses stronger electro-withdrawing effect than other functionalities, indicating that the formation of anion is relatively easy. Thus nIm ligand has the priority to perform bridging mode in the crystal structure. In fact, 2-nitroimidazole always manifests as bidentate mode in all those reported previously.[15] As we know, metal-dicarboxylate system tends to form six-connected M_3 cluster (M = metal)[11a,16a] and four-connected M_2 cluster[16b] instead of three-connected M_2 cluster in 2-D plane. But the 2-D layers of compound **1** consists of six-connected Co_3 and three-connected Co_2 clusters simult-aneously, which is very rare in the metal-dicarboxylate system. Thus, we conclude that the 2-ntroimidazole may act as a template agent in the synthesis of compound **1**. Up to now, including **1**, five Co_3 SBUs have been reported.[11a,16a,17] For compound **1**, each layer includes one-third of Co_{pyra}-Co_{oct}-Co_{pyra} SBUs (pyra = pyramidal coordination, oct = octahedral coordination) and two-third of Co_{tetra}-Co_{oct} SBUs (tetra = tetrahedral coordina-tion), which can be considered as a result of half of the terminal Co atoms of Co_{tetra}-Co_{oct}-Co_{tetra} SBUs have been cut off by three coordinated water molecules.

Crystal structure

Single-crystal analysis shows that compound **1** is a pillared-layer structure based on Co-dicarboxylate layers and nIm pillars, and crystallizes in the orthorhombic system with space group *Cmca*. As shown in Fig. 1a, the 2-D microporous layers of compound **1** composes of two kinds of SBUs—$Co_3(O_2CR)_6$ (SBU-1) and $[Co_2(O_2CR)_3]^+$ (SBU-2). Within the $Co_3(O_2CR)_6$ SBUs, the middle Co(1) atom is coordinated in a CoO_6 manner with four oxygen atoms from four carboxylate groups in mode (μ_4-η^1: η^1: η^1: η^1, Fig. S2, ESI†) and two μ-oxygen atoms from two carboxylate groups in mode (μ_4-η^1: η^1: η^2: η^1). The lengths of Co_{oct}-O bonds are in the range of 2.020(4)-2.174(4)Å (Table 2). The peripheral two Co(2) atoms are bonded with two oxygen atoms from two carboxylate groups in mode I, two oxygen atoms from one carboxylate group in mode II, and one nitrogen atom of the 2-nitroimidazolate ligand as the pillar. In the pyramidal coordination geometry, the centre Co(2) atom is nearly located in the O14-O15-N2-O13 plane (0.441(5)Å from the plane). Similar to other $[Co_3(CO_2)_8]^{2-}$ SBUs,[11a] each Co1-Co2 pair is bridged by one bdc^{2-} carboxylate oxygen atom and two carboxylate groups. The lengths of intra-SBUs Co-Co pair are also listed in Table 2. As for the adjacent $[Co_2(O_2CR)_3]^+$ SBU, which is consisted of a four-coordinated Co(3) and a six-coordinated Co(4). Each Co(3) adopts a CoO_3N coordination mode and is coordinated to two oxygen atoms from two carboxylate groups in mode I, one oxygen atoms from one carboxylate group in mode II and one nitrogen atom from nIm^- ligand. The lengths of Co(3)-O bonds are in the range of 1.933(5)-1.976(5)Å, which are obviously shorter than the Co(4)-O bonds/1.970(4)-2.223(5)Å, while the Co(3)-N(1) /2.035(5)Å is comparable to Co(2)-N(2)/2.044(5)Å. Moreover, the distance between the Co3 atom and the bottom O5-O2-O11 plane is 0.431(2)Å. The Co(4) site holds a CoO_6 mode with slightly distorted octahedral configuration completed by three carboxylate oxygen atoms and three oxygen atoms from three water molecules, since the O-Co-O angles of three axes [174.9(2)-176.3(3)°] approach to 180° (see Table 2). Actually, SBU-1 is an eight-connected node with trinuclear cluster, while SBU-2 is a four-connected node with binuclear cluster in the 3-D network of **1**. In order to predigest the 2-D layer, we view SBU-1 as a six-connected node and SBU-2 as a three-connected node and bdc^{2-} as the linker in the *bc* plane (Fig. 1b). Consequently, the mixed SBUs are linked reciprocally into a 2-D network by the bridging bdc^{2-} as shown in Fig. 1c.

From the view of geometry, the six-connected SBUs such as $Zn_3(\mu\text{-}O_2CR)_6$ SBUs[10c] tend to form triangular channels with side length of ca. 4Å, and the three-connected SBUs tend to form hexagonal channels with dimensions of ca. 20Å. Thus, the

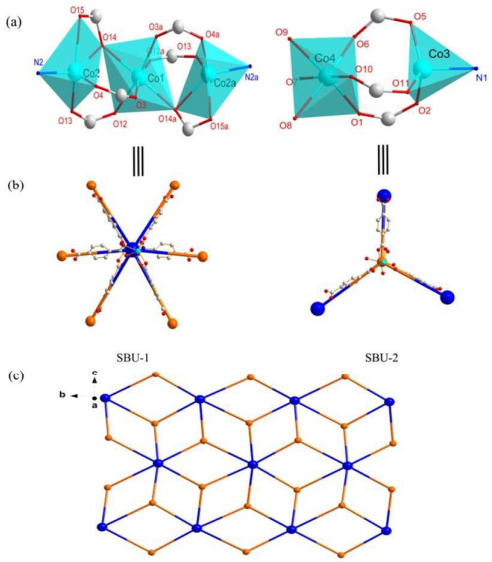

Fig. 1 (a) The coordination environment of Co(II) ions in compound **1**.[Symmetry code: (a) 1/2-x, y, 3/2-z]; (b) Six-connected SBU-1 and three-connected SBU-2 in 2-D layer parallel to the *bc* plane; (c) 2-D Co3-Co2-bdc topological layer.

integration of these two SBUs may lead to a geometrical channel with the dimension between the triangular and hexagonal channels. In fact, among compound **1**, each bridging bdc^{2-} ligand radiates from the $Co_3(O_2CR)_6$ and $[Co_2(O_2CR)_3]^+$ SBUs at about 60° and 120°, respectively, resulting in the construction of 2-D microporous layers network with three types of diamond grids in the *bc* plane. The 2-D layers are further linked into a 3-D framework by nIm ligand, coupled with various channels (Fig. 2a). The first type of channel runs through the *a* axis with diagonal dimensions as long as 11.6×17.9Å^2, while the second type has small opening with diagonal dimension of 9.2×7.1Å^2, and 12.0×2.5Å^2 for the third type, given the van der waals radii of the nearest atoms. Consequently, the combination of different types of SBUs in the constitution of 2-D layers can increase the diversity of channels. To the best of our knowledge, the combination of six-connected and three-connected SBUs applied in the construction of 2-D layers in coordination polymers is unprecedented.

Notably, each SBU-1 infinitely extend along the *c* axis with the bidenate nIm ligand, while the SBU-2 can only extend to one side, and every two neighbouring SBU-2 form a dimer with a nIm ligand. The difference of connective modes between SBU-1 and SBU-2, along with the alternating arrangement of the dimer (half of the SBU-2 connected with the SBU-2 of upper layer, while the other half connected with the lower layer), which contribute to not only the formation of two kinds of channels with two different dimensions (Type IV and Type V with approximate aperture diameter 6.4Å and 5.4Å, respectively) as shown in Fig. 2b, but also ultra-large cages, which are geometrically arranged in a regular fashion (Fig. 3). The maximum diagonal dimension of these polyhedral cages is

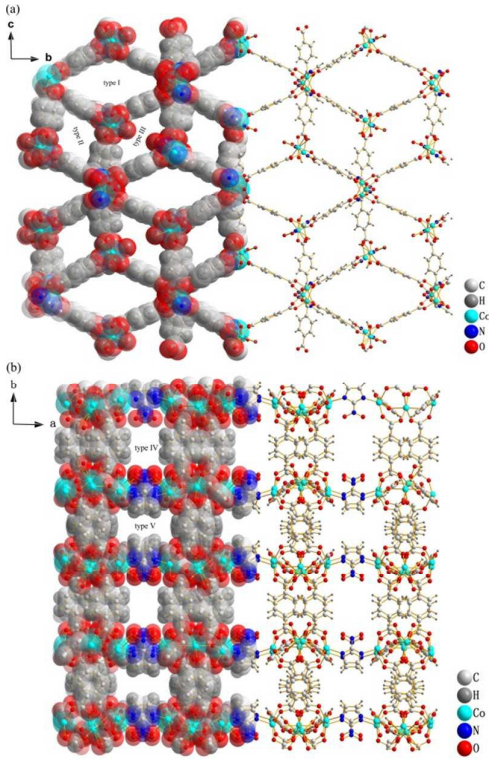

Fig. 2 The 3-D view of the alternating diamond and rectangular channels of **1** along the [1,0,0] direction (a) and [0,0,1] direction (b), respectively.

31.019Å, which has fallen in the scope of the mesoporous. It may account for the large voids of as-synthesized **1**. The total potential solvent-accessible volume is 16,396.1Å^3 for **1**, equal to 61.3% of the unit cell volume, using PLATON.[14] In addition, compared with the aforementioned channels running across *a* axis, the nitro functional group stretching into the type-IV channels can enhance the interaction with CO_2 molecules.

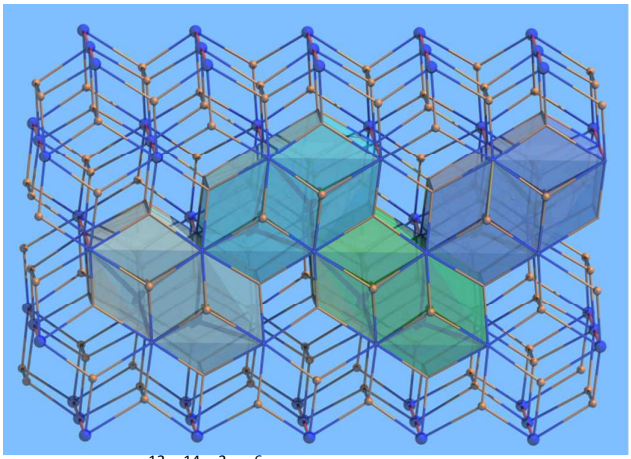

Fig. 3 3-D $\{4^{12}.6^{14}.8^2\}\{4^6\}_2$ topological network along with exclusively polyhedral cages.

Gas sorption study

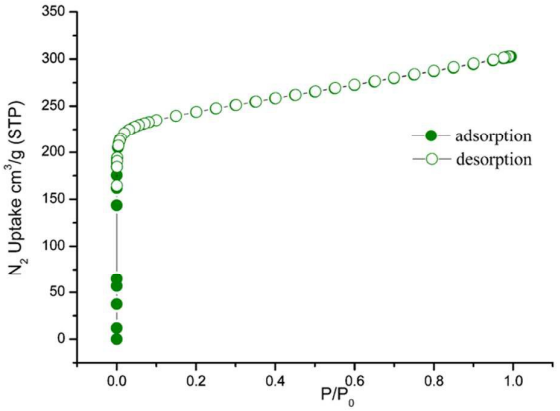

Fig. 4 The N_2 adsorption isotherm of **1** measured at 77K (P/P_0, relative pressure; STP, standard temperature and pressure).

Gas sorption study was conducted on the completely evacuated sample **1**. Before analysis, the sample was soaked in anhydrous acetone for three days with acetone refresh every 8 hours. The permanent porosity of compound **1** is confirmed by N_2 sorption isotherms with the type-I characteristics at 77K, indicating that **1** is a microporous material (Fig. 4). The N_2 Brunauer-Emmett-Teller (BET) surface area and Langmuir surface area are 995m^2/g and 1113m^2/g, respectively (Fig. S3†). The total pore volume was estimated to be 0.47cm^3/g (from N_2 sorption isotherm, 77K), which is less than the 0.72 cm^3/g based on crystal structure. Since the diffusion rate of N_2 molecules into microporous (under 7Å) is very slow at 77K, which prevents N_2 from probing the channels of 6.4Å and 5.4Å.[18a]

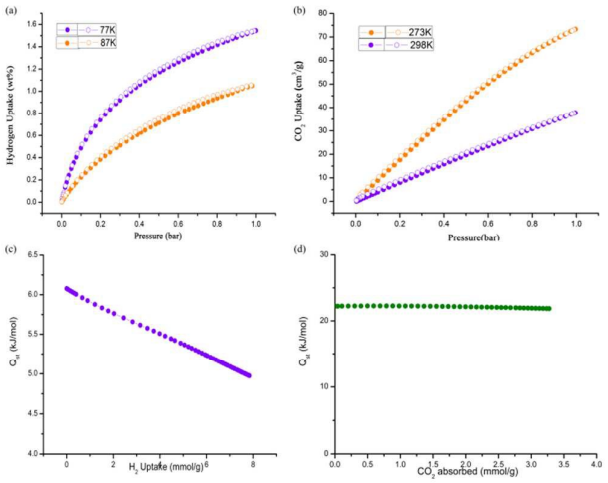

Fig. 5 (a) H_2 adsorption isotherms at 77K and 87K; (b) CO_2 adsorption isotherms at 273K and 298K; (c) H_2 adsorption enthalpy; (d) CO_2 adsorption enthalpy.

As shown in Fig. 5a, the maximum H_2 adsorption of compound **1** at 77K and 1atm is 1.54 wt% (STP, 175.7cm^3/g, 7.84mmol/g), which is obviously higher than those of metal carboxylate boron imidazolate-based assemblies [MC-BIF-2H, 9.9cm^3/g; MC-BIF-3H, 28.2cm^3/g; MC-BIF-5H, 3.7cm^3/g] under the same condition.[2a] The adsorption enthalpy of adsorption was calculated to be 5.5kJ/mol as shown in Fig. 5c. Moreover, sample **1** exhibits high storage capacities of CO_2 at 273K and 298K, which are 73.3cm^3/g (STP, 14.5 wt%, 3.27mmol/g) and 37.7cm^3/g (STP, 7.45 wt%, 1.54mmol/g), respectively (Fig. 5b). To further understand the relationship between the CO_2 uptake capacity and the crystal structure of **1**, the comparisons of characteristic sorption data of compound **1** with 2-nitroimidazolate-based ZIFs and metal carboxylate boron imidazolate-based frameworks (MC-BIF-nH, where n = 2, 3, 5) under the same condition are summarized in Table 3. The introduction of $-NO_2$ functional group, which reveals higher dipole moment than the other functional group, may has a primarily effect on the CO_2 uptake capacity. Because the dipole-quadrupole interactions between the $-NO_2$ functionality and CO_2 can dramatically enhance the adsorption amount of CO_2.[2b] The interaction is further confirmed by the adsorption enthalpy of compound **1** which was calculated from adsorption isotherms measured at 273K and 298K. The zero-coverage adsorption enthalpy value (Q_{st}) of CO_2 is determined to be 22.2kJ/mol (Fig. 5d). Notably, upon increasing the loading, the value (21.9kJ/mol) is nearly unaltered at the maximum loading and is still above the heat of liquefaction of bulk CO_2 (17kJ/mol). The approximately horizontal cure (Fig. 5d) indicates that compound **1** has considerable binding sites for CO_2 uptake.[18b]

Table. 3 Comparison of characteristic sorption data with ZIFs[2b] (including 2-nitroimidazole) and MC-BIF-nH[2a] (n = 2, 3, 5).

	CO_2 uptake (wt %, 273K)	CO_2 uptake (wt %, 298K)	Typical functional group	S_{BET} (m^2/g)
1	**14.5**	**7.45**	**-NO_2**	**995**
ZIF-68	13.1[a]	7.41[b]	-Me	1090
ZIF-69	13.6[a]	8.0[b]	-Cl	950
ZIF-70	10.6[a]	29.5[b]	-H	1730
ZIF-79	10.5[a]	5.8[b]	-Me	810
ZIF-81	12.3[a]	7.53[b]	-Br	760
MC-BIF-2H	10.8	—[c]	-H	—[d]
MC-BIF-3H	7.2	—[c]	-H	—[d]
MC-BIF-5H	1.05	—[c]	-H	—[d]

[a] Approx. Value was taken from SI, 273K/760Torr. [b] Approx. Value was taken from SI, 298K/760Torr. [c] No available data for the gas sorption. [d] No available data for surface area.

The selectivity of CO_2 versus N_2 and CH_4 were predicted from the ration of the initial slopes based on isotherm (Fig. S4 †).[19] At 273K, the CO_2/CH_4 and CO_2/N_2 selectivity for **1** are 3.3 and 14.8, respectively. This further indicates that the polar nitro group has a positive impact on the uptake of CO_2 through enhancing the initial slope of CO_2 isotherm for compound **1**, resulting in greater adsorption enthalpy and CO_2/N_2 selectivity.[19a]

TGA and PXRD analysis

The TGA of compound **1** was collected in the temperature range of 30-600℃, as shown in Fig. S5 (ESI†). The TGA cure

shows three major stages of weight loss, where the initially steep cure of weight loss (25.13%) from 30℃ to 180℃ is associated with the loss of large number of guest molecules (e. g., water or DMF) as well as gas molecules[20a,20b] from the cages and coordinated water molecules(Fig. S6). The endothermic peaks at 61℃ and 180℃ in DSC curve (S5†) confirmed that changes are caused by the lost guest molecules and coordinated water molecules. The relatively high temperature for removing guest molecules may be related to the interaction between the guests and the framework. Subsequently, a major weight loss of compound **1** occurred in the range of 181-311℃, which could be attributed to the decomposition of the nIm ligand (12.44%). The obvious exothermic decomposition peak in DSC curve at 310℃ also reveal that nIm ligands are decomposed from compound **1** in this temperature region.[20c] Subsequently, a major weight loss of compound **1** occurred in the range of 310 – 600℃, which could be attributed to the decomposition of the carboxylate ligand.[20b,20c] The purity of the as-synthesized sample was confirmed by the positive matching of the diffraction peaks between experimental and calculated PXRD patterns (Fig. S8†).

Conclusions

In summary, we have successfully synthesized a new coordination polymer through integrating the diversity of MCFs and the large cage of imidazole in the same framework. The structure reveals not only the diversity and multiplicity of MCFs (such as various types of channels for **1**), but also the high thermal stability of ZIFs. Moreover, the combination of different SBUs in the same 2-D layer can be another way of tuning aperture size for molecular sieving. Additionally, compound **1** exhibits high CO_2 uptake capacity of 14.5 wt%, at 273K/1atm mainly due to the existence of exposed nitro group and uniquely nanometre-sized cages, which is comparable to 13.6 wt% for previously reported ZIF-69 under the same condition. On the basis of the current work, our group is committed to preparing a new family of the porous materials with replacing Co^{2+} ions with other metal ions, or substituting poly-carboxylates ligands for 1,4-benzenedicar-boxylate.

Acknowledgements

This work was supported by the National Science Foundation of China (Grant No. 21173122, 21376124, 21501100 and 21476117).

Notes and references

1 (a) H. Furukawa, K. E. Cordova, M. O'Keeffe and O. M. Yaghi, *Science*. 2013, **341**, 1230444; (b) S. S. Mondal, A. Bhunia, A. Kelling, U. Schilde, C. Janiak and H. J. Holdt, *J. Am. Chem. Soc*. 2014, **136**, 44; (c) S. S. Mondal, A. Bhunia, I. A. Baburin, C. Jäger, A. Kelling, U. Schilde, G. Seifert, C. Janiak and H. J. Holdt, *Chem. Commun.* 2013, **49**, 7599; (d) D. F. Sava, V. C. Kravtsov, F. Nouar, L. Wojtas, J. F. Eubank and M. Eddaoudi, *J. Am. Chem. Soc.* 2008, **130**, 3768.

2 (a) S.-T. Zheng, T. Wu, J. Zhang, M. Chow, R. A. Nieto, P.-Y. Feng and X.-H. Bu, *Angew. Chem. Int. Ed*. 2010, **49**, 5362; (b) R. Banerjee, H. Furukawa, D. Britt, C. Knobler, M. O'Keeffe and O. M. Yaghi, *J. Am. Chem. Soc*., 2009, **131**, 3875; (c) J. J. Perry, J. A. Perman and M. Zaworotko, *J. Chem. Soc. Rev*. 2009, **38**, 1400.

3 (a) M. Pera-Titus, *Chem. Rev.* 2014, **114**, 1413; (b) F. Wang, Z.-S. Lin, H. Yang, Y.-X. Tan and J. Zhang, *Angew. Chem., Int. Ed. Engl*., 2011, **50**, 450; (c) D. F. Sava, M. A. Rodriguez, K. W. Chapman, P. J. Chupas, J. A. Greathouse, P. S. Crozier, T. M. Nenoff, *J. Am. Chem. Soc.*, 2011, **133**, 12398. (d) L.-L. Zhang, Y. Zhang, R.-M. Wang, Z.-X. Kang, X.-B. Lin, D. F. Sun and Q.-G. Meng, *CrystEngComm*, 2012, **15**, 9578.

4 (a) T. Panda, K. M. Gupta, J. W. Jiang and R. Banerjee, *CrystEngComm*, 2014, **16**, 4677; (b) B. Wang, A. P. CÔté, H. Furukawa, M. O'Keeffe and O. M. Yaghi, *Nature*, 2008, 453; (c) C. Wang, L-J. Li, S-F. Tang and X.-B. Zhao, *ACS Appl. Mater. Interfaces*. 2014, **6**, 16932.

5 J. P. Zhang, Y. B. Zhang, J. B. Lin and X. M. Chen, *Chem. Rev*. 2012, **112**, 1001.

6 (a) H. Li, M. Eddaoudi, M. O´Keeffee and O. M. Yaghi, *Nature*, 1999, **402**, 276; (b) K. S. Park, Z. Ni, A. P. Cote, J. Y. Choi, R. Huang, F. J. Uribe-Romo, H. K. Chae, M. O´Keeffe and O. M. Yaghi, *Proc. Natl. Acad. Sci. USA* 2006, 103, 10186.

7 R. Banerjee, A. Phan, B. Wang, C. Knobler, H. Furukawa, M. O'Keeffe and O. M. Yaghi, *Science*, 2008, **319**, 939.

8 (a) J. Olguin and S. Brooker, *Coord. Chem. Rev*. 2011, **13**, 4457; (b) A. Phan, C. J. Dooan, F. J. Uribe-Romo, C. B. Knobler, M. O´Keeffe and O. M. Yaghi. *Acc. Chem. Res*. 2010, **254**, 1918.

9 K.-J. Chen, R.-B. Lin, P.-Q. Liao, C.-T. He, J.-B. Lin, W. Xue, Y.-B. Zhang, J.-P. Zhang, X.-M. Chen, *Cryst. Growth Des.* 2013, **13**, 2118.

10 (a) E. V. Anokhina, M. Vougo-Zanda, X.-Q. Wang and A. J. Jacobson, *J. Am. Chem. Soc*., 2005, **127**, 15000; (b) A. C. Sudik, A. P. Côté and O. M. Yaghi, *Inorg. Chem*., 2005, **44**, 2998; (c) T. Loisean, H. Muguerra, G. Férey, M. Haougs and F. Taulelle, *Journal of Solid Chemistry*, 2005, **178**, 621; (d) N. L. Rosi, J. Kim, M. Eddaoudi, B.-L. Chen, M. O´Keeffee and O. M. Yaghi, *J. Am. Chem. Soc*., 2005, **127**, 1504.

11 (a) F. Luo, Y.-X. Che and J.-M. Zheng, *Crystal Growth Design*, 2009, **9**, 1066; (b) J. Zhang, J.-T. Bu, S.-M. Chen, T. Wu, S.-T. Zhang, Y.-G. Chen, R. A. Nieto, P. Y. Feng and X.-H. Bu, *Angew. Chem. Int. Ed*., 2010, **49**, 8876.

12 T. Panda, K. M. Gupta, J.-W. Jiang and R. Banerjee, *CrystEngComm*, 2014, **16**, 4677.

13 (a) G. M. Sheldrick, SHELXL-97, Program for the Refinement of Crystal Structure, University of Göttingen, Germany, 1997; (b) P. van der Sluis and A. L. Spek, *Acta Crystallogr. Sect. A* 1990, **46**, 194.

14 A. Spek, *J. Appl. Crystallogr*. 2003, **36**, 7.

15 (a) Y.-T. Li, S.-Y. Yao, Y. Wang, K.-H. Cui, H.-Q. Li, X. Wang, J.-Q. Zhu, J. Li and Y.-Q. Tian, *CrystEngComm*, 2011, **13**, 3470; (b) J. Kahr, J. P. S. Mowat, A. M. Z. Slawin, R. E. Morris, D. Fairen-Jimenez and P. A. Wright, *ChemCommun*, 2012, **48**, 6690; (c) B. P. Biswal, T. Panda and R. Banerjee, *ChemCommun*, 2012, **48**, 11868; (d) T. Panda, K. M. Gupta, J.-W. Jiang and R. Banerjee, *CrystEngComm*, 2014, **16**, 4677.

16 (a) X.-F. Wang, Y.-B. Zhang, W. Xue, X.-L. Qi and X.-M. Chen., *CrystEngComm*, 2010, **12**, 3834; (b) M. Eddaoudi, J. Kim, D. Vodak, A. Sudik, J. Wachter, M. O´Keeffe and O. M. Yaghi, *Proc. Natl. Acad. Sci. U.S.A.* 2002, **99**, 4900.

17 R. D. Poulsen, A. Bentien, M. Christensen and B. B. Iversen, *Acta Crystallogr., Sect. B: Struct. Sci.*, 2006, **62**, 245.

18 (a) F. Rodriguez-Reinoso and A. Linares-Solano, In Chemistry and Physics of Carbon; Thrower, P. A., Ed; Markel Dekker: New York, 1988, **21**; (b) D. F. Sava, V. C. Kravtsov, J. Eckert, J.

F. Eubank, F. Nouar and M. Eddaoudi, *J. Am. Chem. Soc*., 2009, **131**, 10394.

19 (a) L.-T. Du, Z.-Y. Lu, K.-Y. Zhang, J.-Y. Wang, X. Zheng, Y. Pan, X.-Z. You and J.-F. Bai, *J. Am. Chem. Soc*. 2013, **135**, 562; (b) J. An, S. J. Geib and N. L. Rosi, *J. Am. Chem. Soc*. 2010, **132**, 38.

20 (a) A. Schejn, L. Balan, V. Falk, L. Aranda, G. Medjahdi and R. Schneider, *CrystEngComm*, 2014, **16**, 4493; (b) L.-T. Cui, Y.-F. Niu, J. Han and X.-L. Zhao, *J. Solid State Chemistry*, 2015, **227**, 155.

Graphical abstract

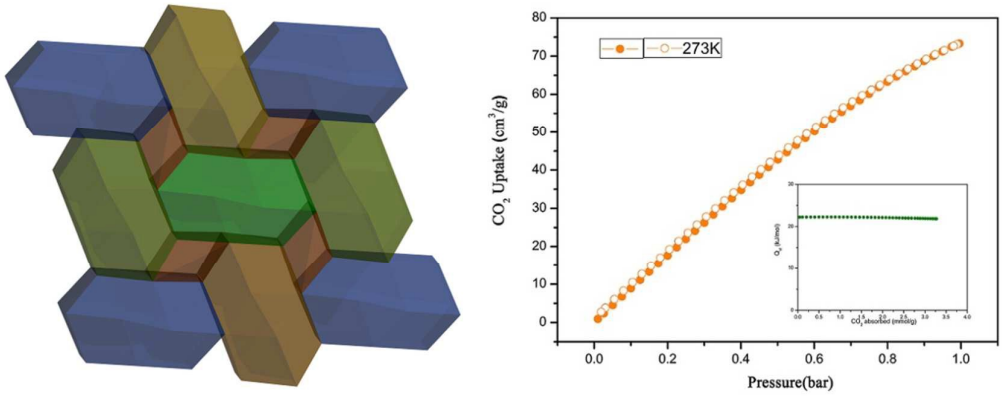

A 3-D pillared-layer metal-organic framework constructed from unprecedented Co_3-Co_2-bdc-based layers and 2-nitroimidazole as pillars exhibits various types of pores, nanometer-sized cavity along with high CO_2 uptake capacity (73.3cm^3/g, at 273K/1atm).